A Passivity Approach to FDTD Stability with Application to Interconnect Modeling

Fadime Bekmambetova, Xinyue Zhang, and Piero Triverio
The Edward S. Rogers Sr. Department of Electrical and Computer Engineering
University of Toronto, 10 King's College Road, Toronto, ON M5S3G4, Canada.
Email: fadime.bekmambetova@mail.utoronto.ca, xinyuezhang.zhang@mail.utoronto.ca, piero.triverio@utoronto.ca

***Abstract*—The application of the Finite Difference Time Domain (FDTD) method to signal and power integrity problems is limited by the large aspect ratio of interconnects and by small skin depth at high frequency, which impose a very fine grid and long simulations. While local grid refinement can be used to overcome this issue, ensuring the stability of the resulting FDTD scheme is not trivial. We present a powerful stability theory for FDTD based on the concept of passivity. The theory is suitable to develop multiresolution FDTD methods with guaranteed stability. A simple and stable subgridding algorithm is derived. Numerical results show its potential for the efficient modeling of skin effect in interconnects.**

***Index Terms*—FDTD, Stability, Passivity, Subgridding.**

I. Introduction

The Finite Difference Time Domain (FDTD) method [1] is commonly chosen for solving Maxwell's equations due to its simplicity and flexibility in setting material properties. Despite these advantages, FDTD can become computationally intensive when applied to interconnects. The minuscule geometrical features and the small skin depth at high frequency may require a significant refinement of the grid in good conductors. Unfortunately, this can dramatically increase the overall computational cost, since a mesh refinement also imposes a reduction in the maximum time step allowed by the Courant-Friedrichs-Lewy (CFL) stability condition [2].

These issues can be ameliorated by the use of local grid refinement, also known as subgridding. However, stability enforcement in subgridding and other complex FDTD methods is a challenging problem. Existing approaches to ensure stability, such as the iteration method [2] and the energy method [3], are based on the analysis of the entire system, which includes fine and coarse grids, as well as the connection between them. This often results in complicated derivations that do not take advantage of the stability of individual grids, which become unstable only when coupled together.

We take a new approach to FDTD stability by leveraging the concept of passivity [4]. Most FDTD setups can be seen as the connection of several *subsystems*, such as grids of different resolution, boundary conditions and lumped models. By ensuring the passivity of each subsystem, we can systematically guarantee the stability of the overall algorithm resulting from their connection [4]. This powerful theoretical framework facilitates the development of complex FDTD algorithms with guaranteed stability, and has been applied to derive a new subgridding scheme with several desirable features: simple implementation, arbitrary refinement ratio and material traverse [4]. In this paper, we investigate the ability of the new subgridding scheme to efficiently model skin effect in copper interconnects, in order to assess its potential for the time-domain analysis of signal and power integrity problems.

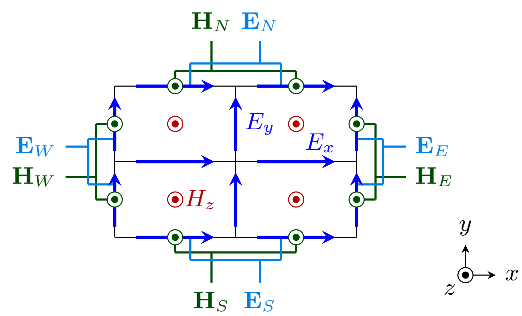

Fig. 1. Two-dimensional region considered in Sec. II.

II. Passivity Theory for FDTD

In this section, we review the novel passivity theory for FDTD and its application to stability analysis [4]. We consider the 2D FDTD region in Fig. 1, and assume a TE mode with components E_x, E_y and H_z. In addition to the standard FDTD field samples, the magnetic field on the outermost edges of the grid is also sampled. These samples, known as hanging variables [5], are used to formulate the update equations for the fields in the region *without* involving any H samples beyond the region boundaries. The hanging variables on each boundary edge are collected into vectors $\mathbf{H}_N^{n+\frac{1}{2}}$, $\mathbf{H}_S^{n+\frac{1}{2}}$, $\mathbf{H}_E^{n+\frac{1}{2}}$ and $\mathbf{H}_W^{n+\frac{1}{2}}$. The FDTD update equations for all E_x, E_y and internal H_z fields can be compactly written as [4]

$$(\mathbf{R}+\mathbf{F})\mathbf{x}^{n+1} = (\mathbf{R}-\mathbf{F})\mathbf{x}^{n} + \mathbf{B}\mathbf{u}^{n+\frac{1}{2}}\,, \tag{1a}$$

$$\mathbf{y}^{n} = \mathbf{L}^T\mathbf{x}^{n}\,, \tag{1b}$$

where

$$\mathbf{x}^n = \begin{bmatrix}\mathbf{E}_x^n\\ \mathbf{E}_y^n\\ \mathbf{H}_z^{n-\frac{1}{2}}\end{bmatrix}, \quad \mathbf{u}^{n+\frac{1}{2}} = \begin{bmatrix}\mathbf{H}_S^{n+\frac{1}{2}}\\ \mathbf{H}_N^{n+\frac{1}{2}}\\ \mathbf{H}_W^{n+\frac{1}{2}}\\ \mathbf{H}_E^{n+\frac{1}{2}}\end{bmatrix}, \quad \mathbf{y}^n = \begin{bmatrix}\mathbf{E}_S^n\\ \mathbf{E}_N^n\\ \mathbf{E}_W^n\\ \mathbf{E}_E^n\end{bmatrix}, \tag{2}$$

are the state, input and output vectors, respectively. Matrix $\mathbf{R}$ depends on permittivities, permeabilities, time step and cell dimensions. Matrix $\mathbf{F}$ is determined by cell dimensions and conductivities. The exact expressions of $\mathbf{R}$, $\mathbf{F}$ and $\mathbf{L}^T$ can be found in [4]. Hanging variables are regarded as inputs while electric fields on the boundary as outputs. Equations (1a)-(1b) thus form an impedance-type model for the electromagnetic fields in the region. For this system to be passive, the following dissipation inequality [6] needs to hold

$$\mathcal{E}(\mathbf{x}^{n+1}) - \mathcal{E}(\mathbf{x}^{n}) \leq s(\mathbf{y}^{n}, \mathbf{u}^{n+\frac{1}{2}}), \quad \forall \mathbf{u}^{n+\frac{1}{2}}, \forall n, \tag{3}$$

where $\mathcal{E}(\mathbf{x}^n) > 0$ is called storage function and describes the energy stored in the region at time n. Supply rate $s(\mathbf{y}^n, \mathbf{u}^{n+\frac{1}{2}})$ instead corresponds to the energy absorbed by the region from the outside world between time n and $n+1$. Following [3], we choose as storage function

$$\mathcal{E}(\mathbf{x}^n) = \frac{\Delta t}{2} \left(\mathbf{x}^n\right)^T \mathbf{R}\mathbf{x}^n, \tag{4}$$

which can be also written as [4]

$$\mathcal{E}(\mathbf{x}^n) = \frac{1}{2} \left(\mathbf{E}_x^n\right)^T \mathbf{D}_{l_x} \mathbf{D}_{l'_y} \mathbf{D}_{\varepsilon_x} \mathbf{E}_x^n + \frac{1}{2} \left(\mathbf{E}_y^n\right)^T \mathbf{D}_{l_y} \mathbf{D}_{l'_x} \mathbf{D}_{\varepsilon_y} \mathbf{E}_y^n + \frac{1}{2} \left(\mathbf{H}_z^{n-\frac{1}{2}}\right)^T \mathbf{D}_A \mathbf{D}_\mu \mathbf{H}_z^{n+\frac{1}{2}}, \tag{5}$$

where $\mathbf{D}_{\varepsilon_x}$, $\mathbf{D}_{\varepsilon_y}$ and $\mathbf{D}_\mu$ are diagonal matrices containing the permittivity and permeability on each edge. Diagonal matrices $\mathbf{D}_{l_x}\mathbf{D}_{l'_y}$, $\mathbf{D}_{l_y}\mathbf{D}_{l'_x}$ and $\mathbf{D}_A$ contain the area of the cells around each field sample. We can clearly see that (5) approximates the total electromagnetic energy stored in the region. As supply rate, we take [4]

$$s(\mathbf{y}^n, \mathbf{u}^{n+\frac{1}{2}}) = \Delta t \frac{\left(\mathbf{y}^n + \mathbf{y}^{n+1}\right)^T}{2} \mathbf{L}^T \mathbf{B} \mathbf{u}^{n+\frac{1}{2}}. \tag{6}$$

One can show that (6) can be rewritten as [4]

$$s = \frac{\Delta t}{2} \left[-\Delta x (\mathbf{E}_S^n + \mathbf{E}_S^{n+1})^T \mathbf{H}_S^{n+\frac{1}{2}} + \Delta x (\mathbf{E}_N^n + \mathbf{E}_N^{n+1})^T \mathbf{H}_N^{n+\frac{1}{2}} + \Delta y (\mathbf{E}_W^n + \mathbf{E}_W^{n+1})^T \mathbf{H}_W^{n+\frac{1}{2}} - \Delta y (\mathbf{E}_E^n + \mathbf{E}_E^{n+1})^T \mathbf{H}_E^{n+\frac{1}{2}} \right]$$

and thus corresponds to the total electromagnetic energy supplied to the region through the North, South, West and East boundaries during one time step Δt.

In [4], we show that with supply rate (6) and storage function (4), system (1a)-(1b) is passive if

$$\mathbf{R} = \mathbf{R}^T > 0, \tag{7a}$$

$$\mathbf{F} + \mathbf{F}^T \geq 0, \tag{7b}$$

$$\mathbf{B} = \mathbf{L}\mathbf{L}^T\mathbf{B}. \tag{7c}$$

Requirement (7a) can be shown to be a generalized CFL condition [4] and, for homogeneous materials, becomes the well known CFL limit $\Delta t < \left(\frac{1}{\varepsilon\mu}\right)^{-\frac{1}{2}} \left(\frac{1}{\Delta x^2} + \frac{1}{\Delta y^2}\right)^{-\frac{1}{2}}$. Condition (7b) requires the conductivity on each edge to be non-negative [4], which is consistent with physical intuition. Requirement (7c) always holds [4]. Conditions (7a)-(7c) provide a powerful method to guarantee FDTD stability.

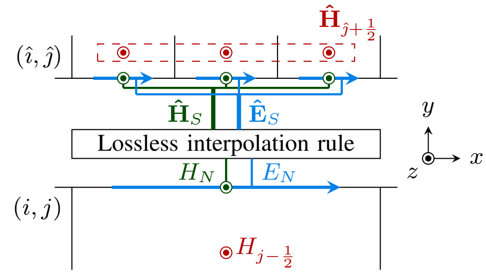

Fig. 2. Interpretation of FDTD subgridding as the connection of three subsystems: coarse mesh, fine mesh, and interpolation rule at the interface.

All subsystems in a given FDTD setup (meshes, boundary conditions, embedded models, ...) are required to satisfy these conditions and be therefore passive. Since the connection of passive systems is passive, it is guaranteed to be stable [7]. A key advantage of the proposed approach is that stability conditions can be applied on each subsystem independently. This feature makes stability proofs simpler, modular and "reusable". Indeed, once some given FDTD models are certified to be passive, they can be interconnected in an arbitrary way with guaranteed stability, without any further proof.

III. Stable Subgridding Scheme

The proposed stability theory was used to derive a simple, stable and effective subgridding method [4]. We can interpret a subgridding scheme as the interconnection of three subsystems: coarse grid, fine grid and the interpolation rule that relates coarsely- and finely-sampled fields at the interface. This viewpoint is illustrated in Fig. 2. As interpolation rule, we use conditions similar to [8], but applied exactly at the coarse-fine interface. The electric field samples on the boundary of the fine grid $\hat{\mathbf{E}}_S$ are made equal to the field sample on the coarse cell boundary, E_N. By reciprocity, the coarse magnetic field on the boundary H_N is instead equated to the average of the magnetic field samples $\hat{\mathbf{H}}_S$ on the fine grid. Under these conditions, we can easily show [4] that the interpolation subsystem is lossless for any Δt. Therefore, for any timestep below the CFL limit of the fine grid, all three subsystems are dissipative, and their connection is thus stable by construction [4].

The proposed subgridding method is straightforward to implement, since all electric and magnetic fields inside the two grids are updated with standard FDTD equations. For the E-field samples at the coarse-fine interface, a simple update equation can be derived by combining the coarse and fine FDTD models (1a)-(1b) with the interpolation rules imposed at the boundary. In this process, the hanging variables are eliminated and one finally obtains [4]

$$E_N^{n+1} = \left(\frac{\varepsilon_x + \frac{\hat{\varepsilon}_x}{r}}{\Delta t} + \frac{\sigma_x + \frac{\hat{\sigma}_x}{r}}{2} \right)^{-1} \left(\frac{\varepsilon_x + \frac{\hat{\varepsilon}_x}{r}}{\Delta t} - \frac{\sigma_x + \frac{\hat{\sigma}_x}{r}}{2} \right) E_N^n + \frac{2}{\Delta y} \left(\frac{\varepsilon_x + \frac{\hat{\varepsilon}_x}{r}}{\Delta t} + \frac{\sigma_x + \frac{\hat{\sigma}_x}{r}}{2} \right)^{-1} \left(\frac{1}{r} \mathbf{T}^T \hat{\mathbf{H}}_{\hat{\jmath}+\frac{1}{2}}^{n+\frac{1}{2}} - H_{j-\frac{1}{2}}^{n+\frac{1}{2}} \right), \tag{8}$$

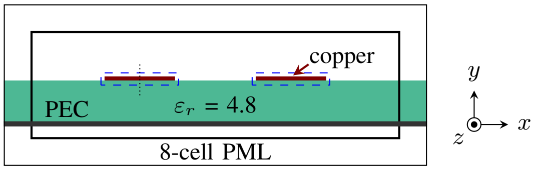

Fig. 3. Structure layout and refined regions (dashed boxes).

Table I
SIMULATION TIMES.

Discretization	Simulation time (s)		
	0.5 GHz	1 GHz	5 GHz
All-fine (r = 9)	8692.5	8653.3	8540.7
All-coarse	13.7	12.6	12.0
Subgridding (r = 5)	153.1	142.9	134.8
Subgridding (r = 9)	472.4	405.9	360.8

where r is the grid refinement ratio and $\mathbf{T}$ is an $r \times 1$ column vector of ones. Quantities ε_x, $\hat{\varepsilon}_x$, σ_x and $\hat{\sigma}_x$ are average permittivity and conductivity values defined in [4]. Once the coarsely-sampled electric field E_N has been updated with (8), the finely-sampled E-fields at the interface are also obtained. This subgridding method is stable by construction, easy to implement and supports material traverse [4]. The grid refinement factor r in (8) can be any positive integer.

IV. Numerical Example

Two copper microstrips are placed on a 0.3 mm-thick dielectric with relative permittivity $\varepsilon_r = 4.8$, as shown in Fig. 3. The microstrips are 0.51 mm wide and 30 μm thick [9]. The 30 μm-thick ground plane is assumed to be a perfect electric conductor (PEC). The microstrips are placed 0.6 mm apart. The 2.7 $\times$ 0.78 mm simulation region is terminated with an 8-cell perfectly matched layer (PML). The structure is excited by a plane wave travelling in the $-y$ direction, with frequency of 0.5 GHz, 1 GHz and 5 GHz. A coarse grid with resolution of 30 μm is used to discretize most of the structure, except for two regions enclosing the conductors, where a refined grid is used to properly resolve the non-uniform current distribution caused by skin effect. The boundaries of the refined regions are one coarse cell away from the microstrips surface, and traverse the dielectric. Two refinement factors of $r = 5$ and $r = 9$ were used. For comparison, we performed an all-fine simulation with full refinement by a factor of 9. All cases were simulated for 4.01 ns. Fig. 4 shows the current density in the left microstrip for different frequencies. The proposed method is able to correctly capture skin effect, which is not resolved by the coarse grid. Table I shows that the proposed method is approximately 20 times faster than a fine FDTD even for the highest refinement factor ($r = 9$). These results confirm the potential of the proposed method for accelerating the time-domain modeling of interconnects and, more generally, multiscale structures.

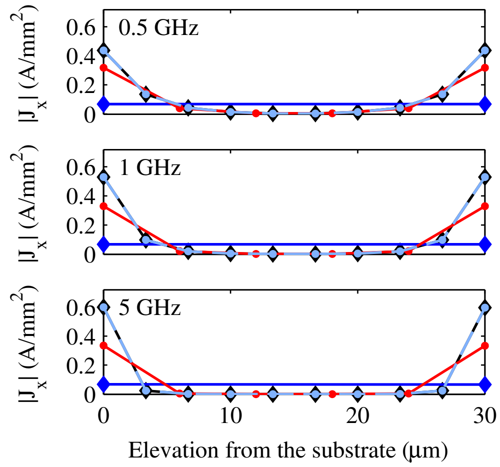

Fig. 4. Current density along the dotted line in Fig. 3 for all-coarse mesh (—◆—), all-fine mesh (—◆—) and the proposed method with r = 5 (—●—) and r = 9 (- -●- -).

V. Conclusion

We presented a passivity theory for FDTD that can be used to systematically ensure stability of both simple and advanced FDTD schemes. The theory was used to develop a new subgridding algorithm with guaranteed stability, support for material traverse and arbitrary grid refinement ratio. A numerical test shows the potential of the proposed developments for the efficient modeling of electromagnetic effects in interconnects and other multiscale structures.

References

[1] K. Yee, "Numerical solution of initial boundary value problems involving Maxwell's equations in isotropic media," *IEEE Trans. Antennas Propag.*, vol. 14, no. 3, pp. 302–307, 1966.

[2] S. D. Gedney, *Introduction to the Finite-Difference Time-Domain (FDTD) Method for Electromagnetics*, 1st ed. San Rafael, CA: Morgan & Claypool Publishers, 2011.

[3] F. Edelvik, R. Schuhmann, and T. Weiland, "A general stability analysis of FIT/FDTD applied to lossy dielectrics and lumped elements," *International Journal of Numerical Modelling: Electronic Networks, Devices and Fields*, vol. 17, no. 4, pp. 407–419, 2004.

[4] F. Bekmambetova, X. Zhang, and P. Triverio, "A dissipative systems theory for FDTD with application to stability analysis and subgridding," *IEEE Trans. Antennas Propag.*, 2016, (submitted).

[5] N. V. Venkatarayalu, R. Lee, Y.-B. Gan, and L.-W. Li, "A stable FDTD subgridding method based on finite element formulation with hanging variables," *IEEE Trans. Antennas Propag.*, vol. 55, no. 3, pp. 907–915, 2007.

[6] C. Byrnes and W. Lin, "Losslessness, feedback equivalence, and the global stabilization of discrete-time nonlinear systems," *IEEE Trans. Autom. Control*, vol. 39, no. 1, pp. 83–98, 1994.

[7] P. Triverio, S. Grivet-Talocia, M. S. Nakhla, F. Canavero, R. Achar, "Stability, causality, and passivity in electrical interconnect models," *IEEE Trans. Adv. Packag.*, vol. 30, no. 4, pp. 795–808, 2007.

[8] L. Kulas and M. Mrozowski, "Reciprocity principle for stable subgridding in the finite difference time domain method," in *EUROCON, 2007. Intl. Conf. "Computer as a Tool"*, Sept 2007, pp. 106–111.

[9] M. Yi, M. Ha, Z. Qian, A. Aydiner, and M. Swaminathan, "Skin-effect-incorporated transient simulation using the Laguerre-FDTD scheme," *IEEE Trans. Microw. Theory Techn.*, vol. 61, no. 12, pp. 4029–4039, Dec 2013.